

Morphology of Single Intracellularly Stained Axons Terminating in Area 3b of Macaque Monkeys

PRESTON E. GARRAGHTY AND MRIGANKA SUR

Department of Brain and Cognitive Sciences, Massachusetts Institute of Technology,
Cambridge, Massachusetts 02139

ABSTRACT

We have studied the morphology of single thalamocortical axons innervating area 3b of postcentral somatosensory cortex in macaque monkeys. We recorded from axons in the white matter below the representation of the hand in postcentral cortex in two monkeys (*Macaca fascicularis*) by using micropipettes filled with horseradish peroxidase (HRP). When an axon was recorded, we delineated its receptive field and determined its modality, and if cutaneous, whether it was slowly or rapidly adapting (SA or RA). We then impaled the axon and injected it with HRP. We recorded and successfully injected many more RA than SA axons, possibly because of differences in their true proportions. The RA axonal arbors varied in mediolateral extent from 350 to 800 μm with a mean of 600 μm . One of the RA axons gave rise to four separate arbors spanning 2.5–3.0 mm of cortex. The single SA axon we recovered was 370 μm in width. We suggest that the individual terminal zones underlie the columnar parcellation of the somatosensory cortex. The presence of arbors spanning several such columns suggests that all regions within the arbor may not be equally effective in driving cortical cells under normal conditions, and such arbors may provide the substrate for a cortical response to alterations in the pattern of input.

Key words: somatosensory cortex; thalamocortical afferents, slowly adapting, rapidly adapting

The region of cortex traditionally referred to as S-I in macaque monkeys is composed of four cytoarchitectonic zones (areas 3a, 3b, 1, 2), and it is now generally agreed that each of these areas contains a separate map of the contralateral skin surface and/or deep tissue (e.g., Merzenich et al., '78; Nelson et al., '80; see Kaas, '83; Kaas and Pons, '88 for reviews). Some data are available regarding other features of the internal organization of these maps, such as areal magnification (Sur et al., '80) and the modular organization of slowly and rapidly adapting afferent inputs (Sur et al., '81, '84). Further, whereas the geometry of thalamocortical inputs has been shown to provide at least a rough substrate for these kinds of topographic and modular features of organization within some cortical fields (e.g., Hubel and Wiesel, '77; Jensen and Killackey, '87), it is also clear that the details of cortical organization depend upon other factors as well. For example, the sizes of receptive fields of cortical neurons have been shown to be alterable by the local application of GABA antagonists (Hicks and Dykes, '83; Dykes et al., '84), and inputs to cortical neurons that are not detected

by using natural stimulation can be revealed by electrical stimulation of peripheral nerves (e.g., Towe et al., '64; Zarzecki and Wiggin, '82). Finally, a good deal is known about the capacity of the representations in areas 3b and 1 to respond to peripheral insults such as nerve cut or digit amputation (Merzenich et al., '83a,b, '84), and, more generally, the map of skin representation in these two cortical areas appears to depend on input activity (Merzenich et al., '88). These observations suggest that some or all of the details of cortical somatotopic maps may derive from the operation of mechanisms that are both dynamic and intrinsic to cortex (e.g., see Kaas et al., '83; Wall and Kaas, '85; Pearson et al., '87; Merzenich et al., '88). Even so, the structure of thalamic afferent inputs to cortex must ultimately

Accepted October 6, 1989.

Address reprint requests to Dr. P.E. Garraghty, Department of Psychology, 301 A & S Psychology Building, Vanderbilt University, Nashville, TN 37240.

constrain both general somatotopic features and the capacity to respond to peripheral perturbations, and few data are available detailing the morphology of thalamocortical afferents. In the present experiments, we have begun to address these issues in macaque monkeys by studying the morphology of single, physiologically characterized thalamocortical fibers arborizing in cortical area 3b. A preliminary report of these data has appeared elsewhere (Garraghty and Sur, '87).

METHODS

Experiments were performed on two adult macaque monkeys. Prior to our terminal experiments, these monkeys had been used in chronic experiments involving recording and stimulation of the superior colliculus and the frontal eye fields in the awake behaving state. The animals were initially anesthetized with an intramuscular injection of ketamine hydrochloride (50 mg/kg), after which we inserted an endotracheal cannula for the delivery of halothane in a 7:3 mixture of nitrous oxide and oxygen. During initial surgery, halothane was delivered at a concentration of 3.5–4.0%. We made a relatively small craniotomy over the lateral somatosensory cortex, exposing the central sulcus and postcentral gyrus representing portions of the hand in areas 3b and 1. After the craniotomy and dural resection, the halothane was reduced to 2.0–2.5% for the remainder of the 10–18 hours of experiments, and a Plexiglas chamber was cemented over the craniotomy. Our recording micropipettes were filled with 5–10% horseradish peroxidase (HRP) in 0.2 M KCl and 0.05 M Tris (pH 7.6) and then beveled to final impedances of 90–110 megohms at 100 Hz. During our experiments, we lowered a micropipette through the somatosensory cortex into the white matter, and the chamber was filled with 3% agar in 0.9% saline and sealed with dental wax to prevent dessication and to reduce recording instability associated with brain pulsations. After the wax had hardened, we slowly advanced the pipette through the white matter until an axon was encountered extracellularly. We then delineated its receptive field and assessed its adaptation properties. Because of the massive acrylic skull cap that secured the recording chambers, stimulation arrays, and

post for fixing the head in the primate chair for the earlier experiments, we were not able to implant stimulating electrodes in the ventroposterior nucleus (VP). Our identification of the axons as thalamocortical was based on the "briskness" of their responses to stimulation of their receptive fields. The laminar locations of the terminations of recovered axons in the cortex suggest that they almost certainly arose from cells in VP (see Results). We then attempted to impale the axon by passing brief current pulses, by advancing the micropipette rapidly in 1–2- μ m steps, or both. Upon successful impalement (signaled by a sharp drop in the DC potential monitored at the pipette tip), we quickly determined that the axon impaled was the same one previously recorded extracellularly, and then injected it iontophoretically with HRP. No less than 2 hours after the last axon was injected, the animals were perfused with a mixture of 2% glutaraldehyde and 1% paraformaldehyde followed by 10%, then 20% sucrose in phosphate buffer. The brains were then extracted and stored overnight in 30% sucrose in phosphate buffer. Brains were sectioned coronally at 100 μ m, and the sections were processed for HRP histochemistry with 3–3' diaminobenzidine with cobalt intensification (Adams, '77). Electrode tracks were reconstructed and recovered axons were identified on the basis of our records of the depths of attempted injections. Recovered axons were reconstructed at 670X over serial sections by using camera lucida.

RESULTS

Data reported here were taken from three hemispheres of two macaque monkeys. In all, we recorded 45 axons in the white matter beneath somatosensory cortex. For each of these axons, we were able to delineate peripheral receptive fields, and we were able to characterize each as being driven by slowly adapting (SA, $N = 9$) or rapidly adapting (RA, $N = 36$) peripheral receptors. Of these, 8 axonal arbors (1 SA and 7 RA) were sufficiently well filled to be completely reconstructed (see Fig. 1). These axonal arbors were confined to cortical area 3b and ramified principally in layer 4. Despite the fact that we were not able to implant stimulating electrodes in VP, these arbors almost certainly arise

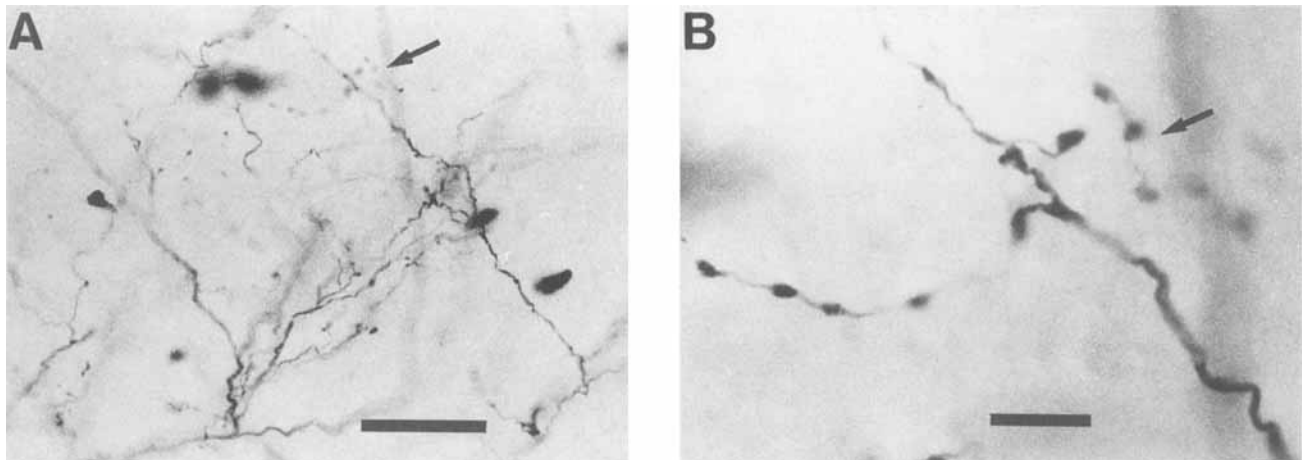


Fig. 1. Photomicrographs of part of the arbor of one of the axons in our sample. The complete reconstruction of this axon's arbor is presented in Figure 3. Arrows in parts A and B point to the same swelling. Note that the swellings generally occur en passant. Scale bar = 50 μ m in A and 10 μ m in B.

from cells in VP. We make this inference because injections of anterograde anatomical tracers into VP of monkeys produce dense label in layer 4 of area 3b (Jones, '75; Jones and Burton, '76; Friedman and Jones, '80; see Jones, '85 for review). There are, of course, other inputs to area 3b that involve layer 4 (e.g., Mesulam et al., '84), but there are no reports of any source of inputs to area 3b which targets layer 4 so specifically (cf., Garraghty et al., '89; see Kaas and Pons, '88).

Figure 2 presents the camera lucida reconstruction of the only SA axon (i.e., an axon with slowly adapting properties) we have recovered. This axon's terminal arbor is relatively small compared to the RA axonal arbors we have recovered (see Fig. 7), and appeared to be restricted to layer 4. At its broadest, it measures only about 370 μm , which is smaller than all but one of the RA arbors we have recovered. Typical of all the axons in our sample, the swellings we assume to be boutons are generally *en passant* (cf. Fig. 1B). These swellings are also not uniformly distributed throughout the axon's terminal field. Rather, there are two vertically oriented clumps that are separated by about 75 μm .

Figure 3 presents the camera lucida reconstruction of the RA axon for which a part of the arbor is shown in Figure 1. Similar to the SA axon illustrated in Figure 2, this arbor is almost completely restricted to layer 4. This RA terminal arbor is among the smallest in our sample, measuring only about 420 μm across. In contrast to the SA arbor shown in Figure 2, this arbor has no obvious gaps but rather is relatively more uniform in its appearance. As for the SA arbor presented in Figure 2, the terminal swellings are almost exclusively *en passant* (see Fig. 1).

Figure 4 presents the camera lucida reconstruction of another RA axonal arbor. In contrast to the arbors presented in Figures 2 and 3, this arbor is much broader; in fact, at about 800 μm , it is the largest single arbor we have seen. Another feature of this arbor, which is characteristic of all the arbors in our sample, is that the boutons are not uniformly distributed throughout the terminal field. Rather, the boutons are much more heavily distributed over about 450 μm within the middle of the arbor with the relatively sparse side branches accounting for the remainder of this arbor's overall width.

Figure 5 illustrates another RA axonal arbor that obviously differs from the ones represented in Figures 3 and 4 in that it has a rather substantial termination in layer 6 in addition to its input to layer 4. The arbor in layer 6 is somewhat sparser than the one in layer 4, and the boutons appear to be more uniformly distributed. It also seems to be "in register" with the arbor in layer 4. An unusual feature of this termination is that the layer 6 arbor does not arise from branches off the parent axon trunk as it passes through layer 6. Rather, the layer 6 arbor is composed of the ramifications of two branches extending down from the layer 4 terminal field (cf. Garraghty et al., '89 for thalamic afferents in somatosensory cortex; and Blasdel and Lund, '83; Florence et al., '83; Florence and Casagrande, '87 for geniculocortical axons). The arbor within layer 4 is about 650 μm wide, but most of the boutons are concentrated within about 400 μm . For this axon, the zone of highest bouton density is not flanked by regions of lower density. Rather, there is only one zone of lower density.

Figure 6 illustrates the most remarkable axon in our sample. This axon elaborates four separate arbors, each largely or completely confined to layer 4. In this flattened view, the total width of this arbor is about 2.5 mm. However, since the

plane of section was oblique with respect to the overall terminal field, 15 sections (1.5 mm) separated the appearance of the lateralmost clump and the disappearance of the arbor on the medial end. Thus the width of this axon's termination is closer to 3.0 mm. The individual clumps range from around 425 μm to nearly 800 μm with the two centrally located clumps being larger than the two on either end.

The widths of all the arbors from our sample are summarized in Figure 7. Note that each of the four clumps of the axon illustrated in Figure 6 is represented separately. On the other hand, we have entered only one value for the SA axon because the gap in its arbor is so small. Overall, the widths of RA arbors ranged between 350 and 800 μm with an average of about 600 μm . As stated earlier, the single SA arbor is about 370 μm wide. In the absence of additional data, however, the conclusion that RA arbors are, on average, wider than SA arbors remains tenuous.

DISCUSSION

We have used intra-axonal recording and labelling with HRP to describe single, physiologically characterized afferents terminating in somatosensory area 3b of macaque monkeys. The axons we have recovered and reconstructed almost certainly arise from the ventroposterior nucleus of the thalamus (see Results; cf. Florence and Casagrande, '87; Garraghty et al., '89). Similar to earlier reports involving the bulk-filling of axons innervating area 3b of owl monkeys (Garraghty et al., '89) and macaques (Conley and Jones, '84), the axon illustrated in Figure 5 demonstrates unequivocally that these axons can have terminations in layer 6. The extent of the arbor in layer 6 for our one axon is much larger than any we have seen in layer 6 of area 3b in owl monkeys and appears to be larger than any recovered by Conley and Jones ('84) based on their brief description. In any event, the large size of this layer 6 arbor certainly implies that it has a substantial influence within layer 6.

The axonal arbors in the present sample also differ in overall size from those previously reported. In owl monkeys, we found that axons in our bulk-filled sample ranged from 100–900 μm in width, but most were under 350 μm (Garraghty et al., '89). Similarly, Conley and Jones ('84) reported that most of the axons in their bulk-filled sample ranged between 200–500 μm in mediolateral width. The axons in the present sample were, on average, larger than in either of those reports. The difference between the present data and those from owl monkeys would most parsimoniously be attributed to the substantial difference in brain size. The difference between our axons and those of Conley and Jones ('84) are not so readily explained. Perhaps our methods bias our sampling toward larger arbors, possibly because larger arbors arise from larger diameter axons that would be more easily recorded by the micropipettes we use. Alternatively, perhaps our methods fill axonal arbors more completely. Whatever the case, much more data will be required before authoritative normative statements on arbor size will be possible.

Comparisons with afferents to area 17: laminar and modular organization

The RA arbors we have recovered are, on average, larger than the single SA arbor in our sample. However, with only a single SA afferent, reliable comparisons between SA and RA afferents cannot be made. Nevertheless, it is possible that as our sample size increases, SA and RA fibers will be found to

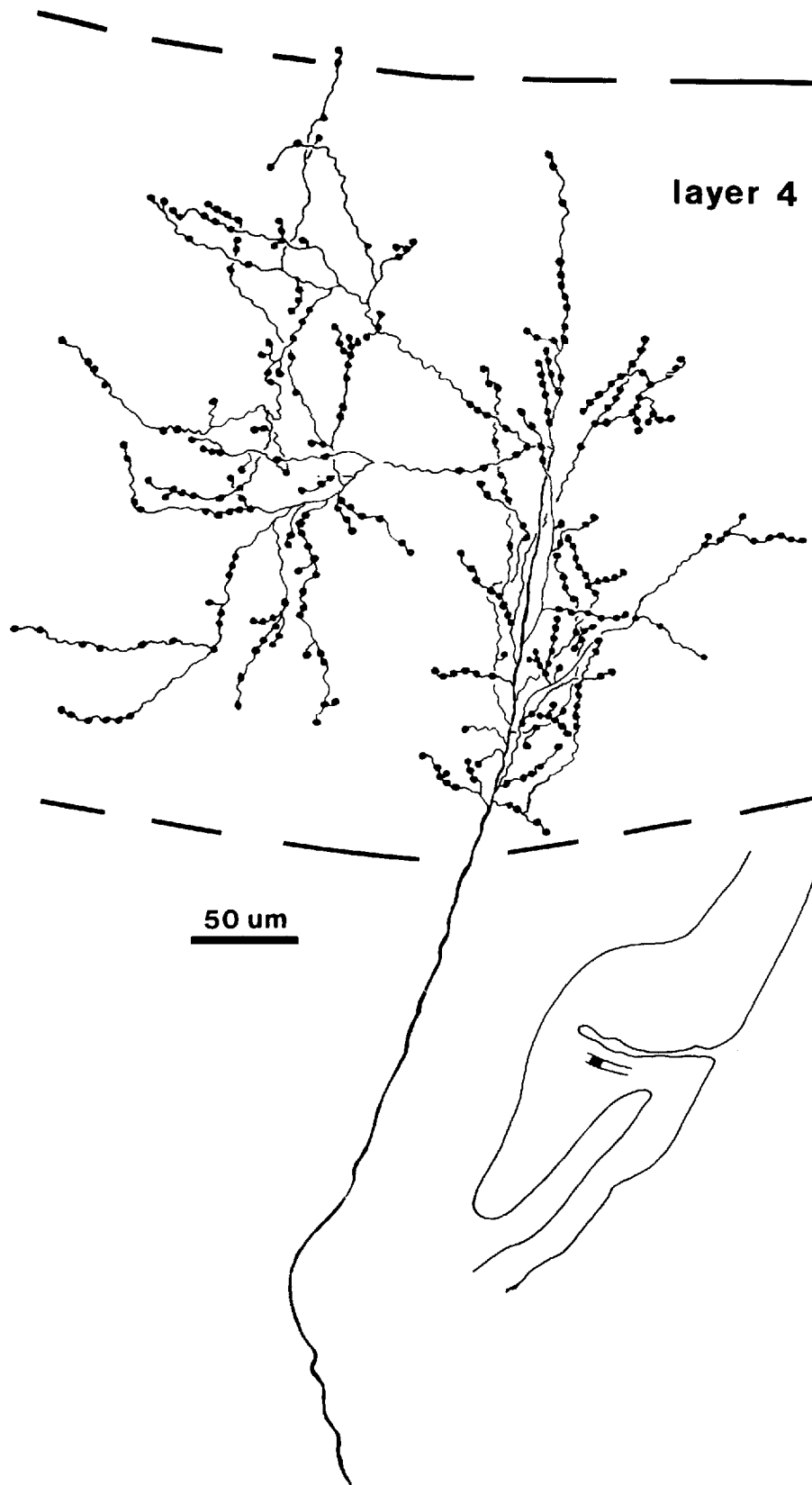


Fig. 2. A slowly adapting afferent terminating in layer 4. This axon's terminal arbor is relatively small compared to those displayed in subsequent figures. It was recorded and injected at a depth of 5,000 μm below the cortical surface. Its receptive field was located on the glabrous radial distal phalange of digit 1. Typical of all of the axons we have recovered, the swellings that we assume to be boutons generally occur en passant. Scale bar = 50 μm .

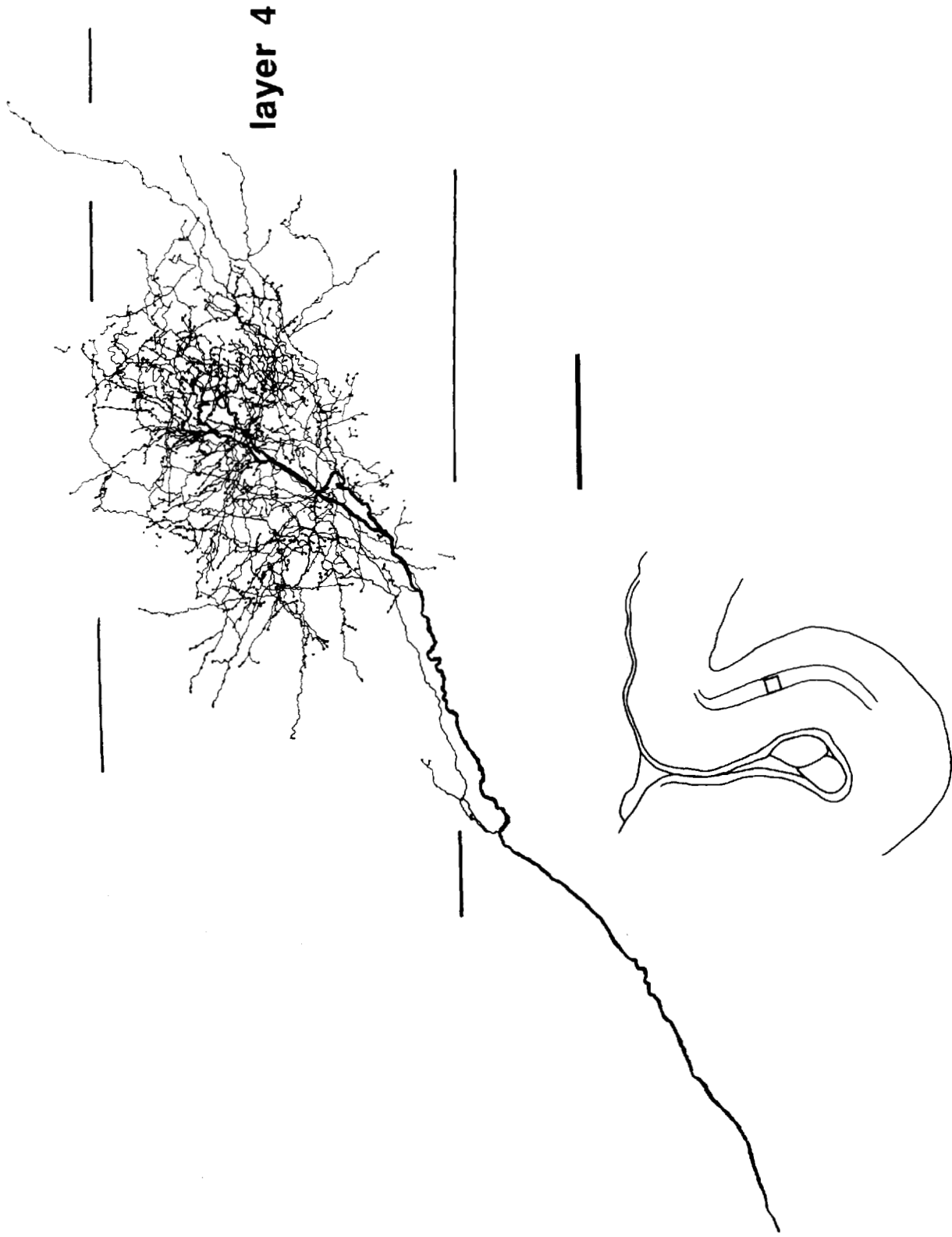


Fig. 3. A rapidly adapting afferent terminating in area 3b. This axon's arbor is, at about 420 μm , one of the smaller RA arbors in our sample. It was recorded and injected at a depth of 3,628 μm below the cortical surface. Its receptive field was on the dorsal surface of the proximal phalanges of digits 3 and 4. Scale bar = 100 μm .

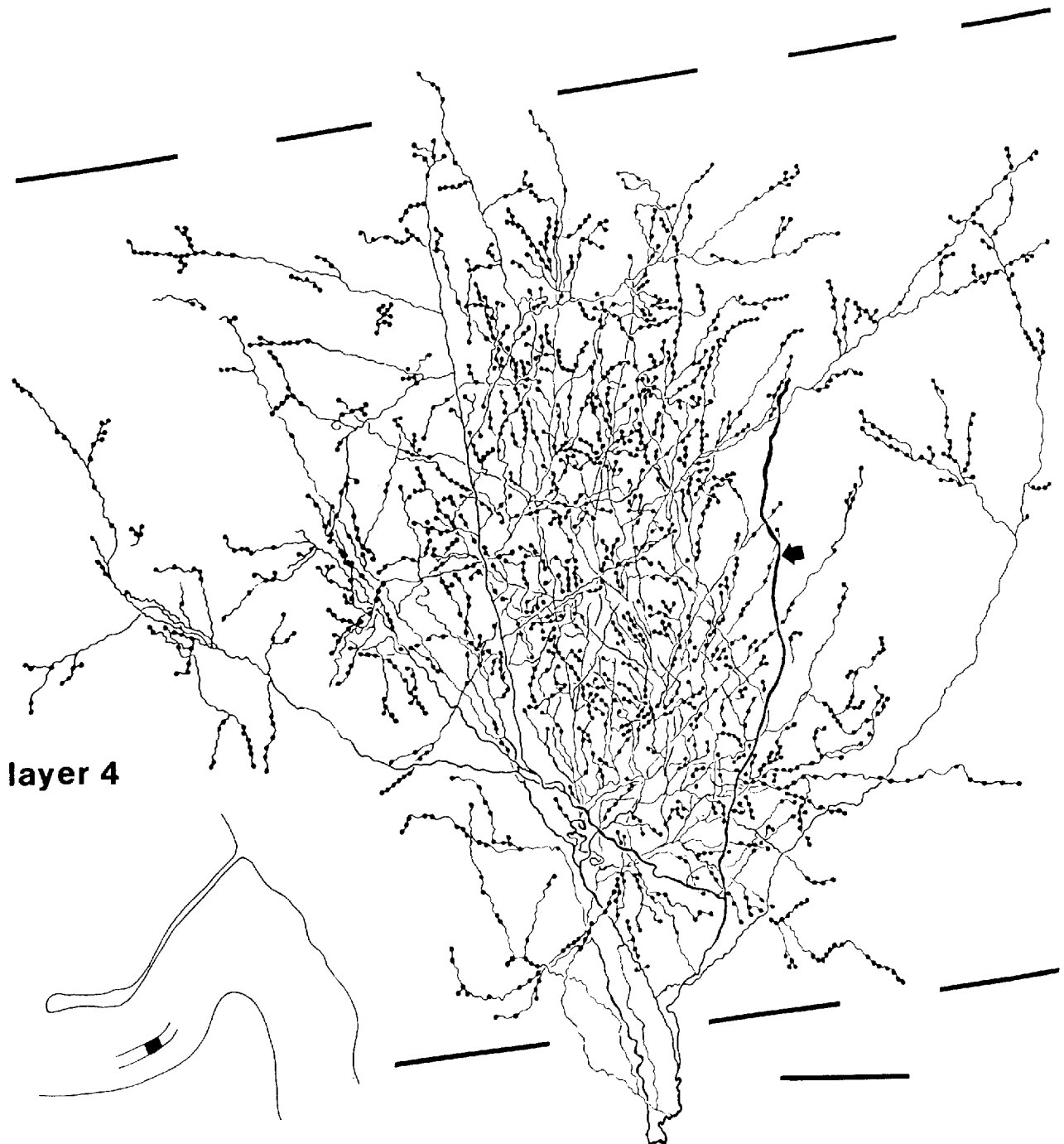


Fig. 4. Another rapidly adapting afferent terminating in layer 4. This axon was recorded and injected 5,148 μm below the cortical surface. This arbor is about 800 μm wide, and is the largest single clump in our sample. Its receptive field was located on the hypothenar pad of the palm. The arrow points to the axon at the location of the injection site.

Whereas the axon appears in the midst of the arbor, this is an artifact associated with reconstruction over serial sections. The injection site was in the white matter several sections removed from the terminal arbor. Scale bar = 100 μm .

have arbors differing in their extents, as appears to be the case, for example, with parvicellular and magnocellular afferents to visual cortex (e.g., Blasdel and Lund, '83; Florence and Casagrande, '87).

We report here on only 8 axons, 7 of which were RA. This is a reasonable reflection of our total sample of recorded,

cutaneously responsive axons (45 recorded; 36 RA and 9 SA). This bias toward recording (and injecting) RA axons could reflect the true proportions of these classes of thalamocortical afferents to area 3b (cf. Johansson and Vallbo, '79). A comparable asymmetry in the proportional representation of functional thalamocortical input classes exists in

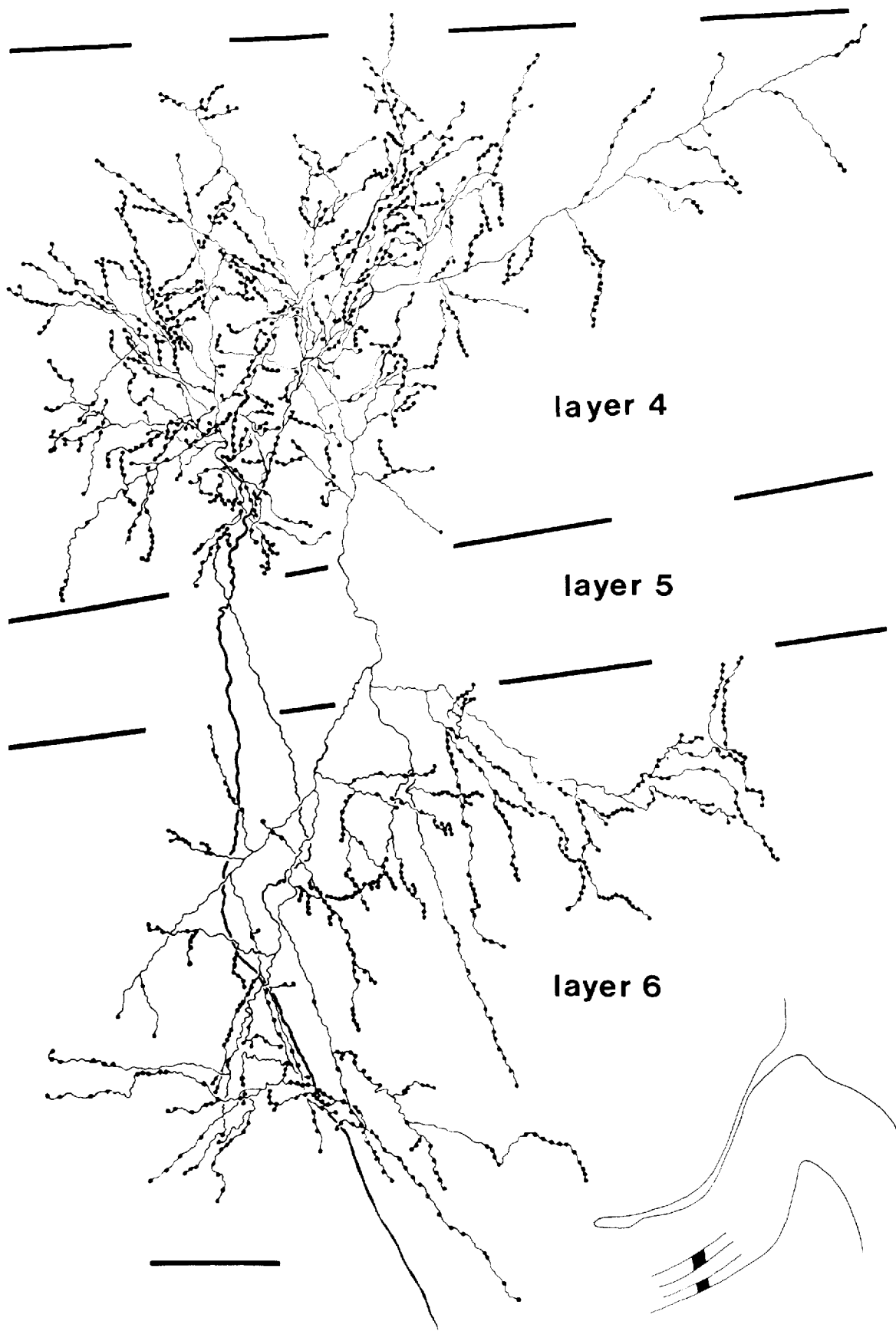


Fig. 5. An example of a rapidly adapting afferent with terminations in layers 4 and 6. This axon was recorded and injected at a depth of $6,573 \mu\text{m}$ from the cortical surface. Its receptive field was on the dorsum of the fifth digit extending across the middle and distal phalanges. Scale bar – $100 \mu\text{m}$.



Fig. 6. An example of a rapidly adapting afferent with multiple terminations in area 3b. This axon was recorded and injected $7,007 \mu\text{m}$ beneath the cortical surface. Its receptive field was on the lateral surface of the face. The widths of the individual clumps of this arbor are reflected in Figure 7, but the overall width of this axon's terminal field in this flattened view (outside edge to outside edge) is 2.47 mm . Scale bar = $200 \mu\text{m}$.

the macaque geniculocortical system; here, however, parvocellular inputs to cortex outnumber magnocellular inputs by a considerable amount (e.g., Livingstone and Hubel, '88). Alternatively, it remains possible that SA fibers are finer in diameter than RA fibers and we may have undersampled SA afferents because of an electrode sampling bias in favor of larger caliber fibers.

In the primate visual cortex, geniculocortical afferents arising from cells in parvocellular laminae have a different sublaminar pattern of termination than inputs from cells in magnocellular laminae (e.g., Blasdel and Lund, '83; Florence and Casagrande, '87). We have seen no evidence for any comparable segregation within our sample. The bulk-filling of axons in both owl monkeys (Garraghty et al., '89) and macaque monkeys (Conley and Jones, '84) also failed to reveal any sublaminar preferences among presumptive thalamocortical axons.

Although we have no direct evidence that SA and RA afferents are segregated horizontally in area 3b, evidence does exist in support of modular organization. Sur et al. ('81, '84) used extracellular recordings to demonstrate that SA and RA inputs to area 3b are not randomly distributed, but rather are organized into "bands" reminiscent of ocular dominance columns in visual cortex. That the thalamic input to area 3b serves as the anatomical underpinning of this modular organization was suggested by the observation that the SA and RA columns were evident only in middle cortical layers; in supra- and infragranular layers all responses were transient (i.e., RA-like). Moreover, based on the extracellular recordings, the SA and RA columns varied between 200 and 600 μm (Sur et al., '81), a range that may be very consistent with the widths of arbors reported here (see the next section). Presumably, the individual clumps of the axon illustrated in Figure 6 ramify in 4 separate RA columns separated by intervening SA bands. Such columnar specificity was shown elegantly by Blasdel and Lund ('83) who combined the transneuronal transport of intraocularly injected anatomical tracer with intracellular filling of geniculocortical afferents in a macaque monkey. They showed that each arbor of an individual afferent with multiple clumps was restricted to an ocular dominance column appropriate for the eye of origin (cf. Landry et al., '82). As suggested previously, therefore, the SA/RA banding in primate area 3b may well share features in common with ocular dominance segregation in primary visual cortex (Sur et al., '84).

Are all parts of an axon's arbor equally effective?

The axon with multiple arbors spanned 2.5–3.0 mm of cortex. Yet studies of magnification factors in the hand region of somatosensory cortex (of owl monkeys) have suggested that a "hypercolumn" extends over a distance of only 1–1.5 mm (Sur et al., '80). If one can in fact move 500–750 μm in any direction in area 3b and record neurons with completely nonoverlapping receptive fields, and if axons such as the one shown in Figure 4 are common, then one could conclude that all parts of an axon's terminal field are not equally effective in driving postsynaptic activity. In general, this conclusion might well also apply to each of the individual arbors within this axon's terminal field and to the remaining arbors in our sample also. We noted that the arbors could generally be characterized as having a higher bouton density in a central core zone flanked by regions of lower density. If one makes the simplifying assumption that regional variations in bouton density within an axon's ter-

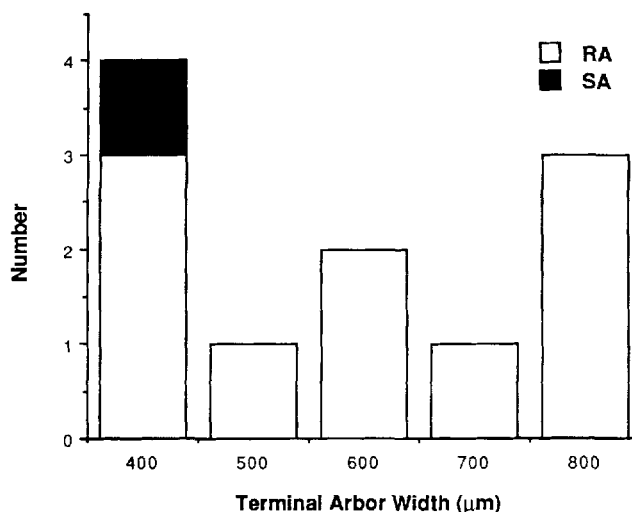


Fig. 7. Histograms presenting terminal arbor widths for the axons recovered thus far. Values represented on the abscissa reflect the mid-points of bins $\pm 50 \mu\text{m}$. No attempt has been made to correct for tissue shrinkage. The individual clumps of the axon illustrated in Figure 6 are represented separately. The arbor widths of the rapidly adapting (RA) afferents ranged from 350 to 800 μm with a mean of 600 μm . The single slowly adapting (SA) afferent was 370 μm in width. These values agree fairly closely with those previously reported in owl monkeys using bulk-filling procedures (Garraghty et al., '89).

minal field are related in a more or less direct way with its "sphere of influence" (cf. Garraghty et al., '89), with the recognition that other factors also play a role in "synaptic efficacy" (e.g., Burke, '87), then one can imagine that variations in effectiveness exist within the single arbors as well. So, for example, the layer 4 termination of the axon illustrated in Figure 3 had a total width of about 650 μm with a region of higher density measuring only about 400 μm . Since it seems reasonable that the thalamocortical afferents to area 3b are the anatomical subunits underlying its functional post-synaptic organization, estimates of SA and RA column widths as well as cortical magnification are both more consistent with the widths of the high-density parts of arbors rather than the total arbor widths. That all parts of an axonal arbor might not be equally effective (or even active) is not a novel idea (e.g., Parnas, '72; Smith, '80; Henneman et al., '84; cf. Swindale and Cynader, '86; Landry et al., '87), but it is one that merits serious consideration as one attempts to make sense of functional topography in cortex based on information regarding afferent structure.

Relationship of single axon arbors to cortical plasticity

Related to the issue of whether all parts of an axon's arbor are equally effective (or active) at all times is the question of whether inferences can be drawn from these data regarding the mechanisms of neural plasticity. In adult monkeys that undergo lesions of peripheral nerves, functional reorganization occurs within the somatotopic map in somatosensory cortex (see Kaas et al., '83 for review). In the somatosensory cortex, some of the reorganization is evident immediately (e.g., Merzenich et al., '83b), and some emerges over time (e.g., Merzenich et al., '83a). This latter form of plasticity, reorganization emerging after a period of time, has now become a common observation. For example, photocoagula-

tion lesions of small areas on the retina initially denervate corresponding loci in the lateral geniculate nucleus and visual cortex. As little as 1 month after such lesions, however, responsiveness recovers in the "denervated" part of the cat lateral geniculate nucleus (e.g., Eysel et al., '81), and in the affected portion of primary visual cortex of cats (Chino et al., '89) and monkeys (Heinen and Skavenski, '88). Importantly, the area of "recovery" is circumscribed such that silent regions remain after large denervations. The mechanisms behind short-term and long-term reorganization might differ, with short-term recovery involving "unmasking" of pre-existing inputs and long-term recovery possibly involving "sprouting" of inputs to new territories. Evidence for sprouting in the mature brain, however, remains inconclusive at best, and it is parsimonious at present to attribute both kinds of reorganization to "unmasking" (Kaas et al., '83; Merzenich et al., '88; Killackey, '89). Perhaps ineffective regions of an axon's arbor attain efficacy when the normally prepotent inputs are eliminated (e.g., Merrill and Wall, '72; Rhoades et al., '87). The size of arbors, then, sets the distance limit for reorganization at least at the level of cortex. The maximal extent of cortex that reorganizes after removal of a subset of inputs is about 2 mm (Merzenich et al., '83b), which is comparable in size to the largest arbor we have observed (Fig. 6). Finally, if our sample of axons is somewhat representative, and SA and RA afferents do differ dramatically in size and in the likelihood of having multiple arbors, then the capacity for reorganization after injury might be modality-specific such that the RA subsystem provides the basis for larger scale reorganization than the SA subsystem.

ACKNOWLEDGMENTS

We thank Drs. S.L. Florence, A. Morel, and T.P. Pons for helpful comments on an earlier version of this manuscript, and Drs. L.A. Krubitzer, M.G. MacAvoy, and R. Fischer for excellent technical assistance. The monkeys were generously provided by Dr. C.J. Bruce. This work was supported by NS07497 (P.E.G.) and NSF Grant BNS 8411973 (M.S.).

LITERATURE CITED

- Adams, J.C. (1977) Technical considerations on the use of horseradish peroxidase as a neuronal marker. *Neuroscience* 2:141-145.
- Blasdel, G.G., and J.S. Lund (1983) Termination of afferent axons in macaque striate cortex. *J. Neurosci.* 3:1389-1413.
- Burke, R.E. (1987) Synaptic efficacy and the control of neuronal input-output relations. *Trends Neurosci.* 10:42-45.
- Chino, Y., A. Langston, J.H. Kaas, and L.A. Krubitzer (1989) Evidence that retinal lesions induce retinotopic reorganization in visual cortex of adult cats. *Invest. Ophthalmol. Vis. Sci., Suppl.* 30:112 (Abstr.).
- Conley, M., and E.G. Jones (1984) Laminar terminations of individual afferent axons in SI cortex in *Macaca*. *Proc. Soc. Neurosci.* 10:495 (Abstr.).
- Dykes, R.W., P. Landry, R. Metherate, and T.P. Hicks (1984) Functional role of GABA in cat primary somatosensory cortex: Shaping receptive fields of cortical neurons. *J. Neurophysiol.* 52:1066-1093.
- Eysel, U.T., F. Gonzalez-Aguilar, and U. Mayer (1981) Time-dependent decrease in the extent of visual deafferentation in the lateral geniculate nucleus of adult cats with small retinal lesions. *Exp. Brain Res.* 41:256-263.
- Florence, S.L., and V.A. Casagrande (1987) Organization of individual afferent axons in layer IV of striate cortex in a primate. *J. Neurosci.* 7:3850-3868.
- Florence, S.L., M.A. Sesma, and V.A. Casagrande (1983) Morphology of geniculostriate afferents in a prosimian primate. *Brain Res.* 270:127-130.
- Friedman, D.P., and E.G. Jones (1980) Focal projections of electrophysiologically defined groupings of thalamic cells on the monkey somatic sensory cortex. *Brain Res.* 191:249-252.
- Garraghty, P.E., and M. Sur (1987) The morphology of single physiologically identified thalamocortical axons innervating somatosensory cortex in macaque monkeys. *Proc. Soc. Neurosci.* 13:471 (Abstr.).
- Garraghty, P.E., T.P. Pons, M. Sur, and J.H. Kaas (1989) The arbors of axons terminating in middle cortical layers of somatosensory area 3b in owl monkeys. *Somatosens. Motor Res.* 6:401-411.
- Heinen, S.J., and A.A. Skavenski (1988) Recovery of visual driving in the foveal projection of striate cortex following bilateral foveal ablation in adult monkey. *Invest. Ophthalmol. Vis. Sci., Suppl.* 29:23 (Abstr.).
- Henneman, E., H.-R. Luscher, and J. Mathis (1984) Simultaneously active and inactive synapses of single Ia fibres on cat spinal motoneurons. *J. Physiol.* 352:147-161.
- Hicks, T.P., and R.W. Dykes (1983) Receptive field size for certain neurons in primary somatosensory cortex is determined by GABA-mediated intracortical inhibition. *Brain Res.* 274:160-164.
- Hubel, D.W., and T.N. Wiesel (1977) Functional architecture of macaque monkey visual cortex. *Proc. R. Soc. Lond. B* 198:1-59.
- Jensen, K.F., and H.P. Killackey (1987) Terminal arbors of axons projecting to the somatosensory cortex of the adult rat. I. The normal morphology of specific thalamocortical afferents. *J. Neurosci.* 7:3529-3543.
- Johansson, R.S., and A.B. Vallbo (1979) Tactile sensibility in the human hand: relative and absolute densities of four types of mechanoreceptive units in glabrous skin. *J. Physiol.* 286:283-300.
- Jones, E.G. (1975) Lamination and differential distribution of thalamic afferents within the sensory-motor cortex of the squirrel monkey. *J. Comp. Neurol.* 160:167-204.
- Jones, E.G. (1985) Connectivity of the primate sensory-motor cortex. In E.G. Jones and A. Peters (eds): *Cerebral Cortex*, Vol. 5, *Sensory-Motor Areas and Aspects of Cortical Connectivity*. New York: Plenum, pp. 113-183.
- Jones, E.G., and H. Burton (1976) Areal differences in the laminar distributions of thalamic afferents in cortical fields of the insular, parietal and temporal regions of primates. *J. Comp. Neurol.* 168:197-248.
- Kaas, J.H. (1983) What, if anything, is S-I? The organization of the "first somatosensory area" of cortex. *Physiol. Rev.* 63:206-231.
- Kaas, J.H., and T.P. Pons (1988) The somatosensory system of primates. In H.D. Steklis and J. Erwin (eds): *Comparative Primate Biology*, Vol. 4, *Neurosciences*. New York: Alan R. Liss, pp. 421-468.
- Kaas, J.H., M.M. Merzenich, and H.P. Killackey (1983) Changes in the organization of somatosensory cortex following peripheral nerve damage in adult and developing mammals. *Ann. Rev. Neurosci.* 6:325-356.
- Killackey, H.P. (1989) Static and dynamic aspects of cortical somatotopy: A critical evaluation. *J. Cog. Neurosci.* 1:3-11.
- Landry, P., J. Villemure, and M. Deschênes (1982) Geometry and orientation of thalamocortical arborizations in the cat somatosensory cortex as revealed by computer reconstruction. *Brain Res.* 237:222-226.
- Landry, P., P. Diadori, S. Leclerc, and R.W. Dykes (1987) Morphological and electrophysiological characteristics of somatosensory thalamocortical axons studied with intra-axonal staining and recording in the cat. *Exp. Brain Res.* 65:317-330.
- Livingstone, M.S., and D.H. Hubel (1988) Do the relative mapping densities of the magno- and parvocellular systems vary with eccentricity? *J. Neurosci.* 8:4334-4339.
- Merrill, E.G., and P.D. Wall (1972) Factors forming the edge of a receptive field: the presence of relatively ineffective afferent terminals. *J. Physiol.* 226:825-846.
- Merzenich, M.M., J.H. Kaas, M. Sur, and C.-S. Lin (1978) Double representation of the body surface within cytoarchitectonic areas 3b and 1 in "S-I" in the owl monkey (*Aotus trivirgatus*). *J. Comp. Neurol.* 181:41-74.
- Merzenich, M.M., J.H. Kaas, J. Wall, R.J. Nelson, M. Sur, and D. Felleman (1983a) Topographic reorganization of somatosensory cortical areas 3b and 1 in adult monkeys following restricted deafferentation. *Neuroscience* 8:33-55.
- Merzenich, M.M., G. Recanzone, W.M. Jenkins, T.T. Allard, and R.J. Nudo (1988) Cortical representational plasticity. In P. Rakic and W. Singer (eds): *Neurobiology of Neocortex*. New York: John Wiley and Sons, pp. 41-67.
- Merzenich, M.M., J.H. Kaas, J.T. Wall, M. Sur, R.J. Nelson, and D.J. Felleman (1983b) Progression of changes following median nerve section in the cortical representation of the hand in areas 3b and 1 in adult owl and squirrel monkeys. *Neuroscience* 10:639-665.
- Merzenich, M.M., R.J. Nelson, M.P. Stryker, M.S. Cynader, A. Schoppmann, and J.M. Zook (1984) Somatosensory cortical map changes following digit amputation in adult monkeys. *J. Comp. Neurol.* 224:591-605.
- Mesulam, M.-M., A.D. Rosen, and E.J. Mufson (1984) Regional variations in cortical cholinergic innervation: Chemoarchitectonics of acetylcholinesterase-containing fibers in the macaque brain. *Brain Res.* 311:245-258.

- Nelson, R.J., M. Sur, D.J. Felleman, and J.H. Kaas (1980) Representations of the body surface in postcentral parietal cortex of *Macaca fascicularis*. *J. Comp. Neurol.* 192:611–643.
- Parnas, I. (1972) Differential block at high frequency of branches of a single axon innervating two muscles. *J. Neurophysiol.* 35:903–914.
- Pearson, J.C., L.H. Finkel, and G.M. Edelman (1987) Plasticity in the organization of adult cerebral cortical maps: A computer simulation based on neuronal group selection. *J. Neurosci.* 7:4209–4233.
- Rhoades, R.W., G.R. Belford, and H.P. Killackey (1987) Receptive-field properties of rat ventral posterior medial neurons before and after selective kainic acid lesions of the trigeminal brain stem complex. *J. Neurophysiol.* 57:1577–1600.
- Smith, D.O. (1980) Mechanisms of action potential propagation failure at sites of axon branching in the crayfish. *J. Physiol.* 301:243–259.
- Sur, M., M.M. Merzenich, and J.H. Kaas (1980) Magnification, receptive-field area, and “hypercolumn” size in areas 3b and 1 of somatosensory cortex in owl monkeys. *J. Neurophysiol.* 44:295–311.
- Sur, M., J.T. Wall, and J.H. Kaas (1981) Modular segregation of functional cell classes within the postcentral somatosensory cortex of monkeys. *Science* 212:1059–1061.
- Sur, M., J.T. Wall, and J.H. Kaas (1984) Modular distribution of neurons with slowly adapting and rapidly adapting responses in area 3b of somatosensory cortex in monkeys. *J. Neurophysiol.* 51:724–744.
- Swindale, N.V., and M.S. Cynader (1986) Physiological segregation of geniculate-cortical afferents in the visual cortex of dark-reared cats. *Brain Res.* 362:281–286.
- Towe, A.L., H.D. Patton, and T.T. Kennedy (1964) Response properties of neurons in the pericruciate cortex of the cat following electrical stimulation of the appendages. *Exp. Neurol.* 10:325–344.
- Wall, J.T., and J.H. Kaas (1985) Cortical reorganization and sensory recovery following nerve damage and regeneration. In C.W. Cotman (ed): *Synaptic Plasticity*. New York: Guilford, pp. 231–260.
- Zarzecki, P., and D.M. Wiggan (1982) Convergence of sensory inputs upon projection neurons of somatosensory cortex. *Exp. Brain Res.* 48:28–42.